Instrumented Tensile and Falling Weight Impact Response of Injection-Molded α- and β-Phase Polypropylene Homopolymers with Various Melt Flow Indices

J. KARGER-KOCSIS,[1] D. E. MOUZAKIS,[1] G. W. EHRENSTEIN,[2] J. VARGA[2,3]

[1] Institut für Verbundwerkstoffe GmbH, Universität Kaiserslautern, Pf. 3049, D-67653 Kaiserslautern, Germany

[2] Lehrstuhl für Kunststofftechnik, Universität Erlangen-Nürnberg, D-91058 Erlangen-Tennenlohe, Germany

[3] Department of Plastics and Rubber Technology, Technical University of Budapest, H-1111 Budapest, Hungary

Received 29 July 1998; accepted 16 October 1998

ABSTRACT: In this study the instrumented tensile (ITI) and falling weight impact (IFWI) behavior of injection-molded α- and β-phase polypropylene (PP) homopolymers were compared at ambient temperature in a broad melt flow index (MFI = 0.7–13 dg/min) range. It was found that the toughness of β-PP is superior to the α-PP: the difference between them increased with decreasing MFI or increasing molecular weight (MW). As expected, the injection molding induced skin layer thickness increased with increasing MW. Effects of the skin-core morphology were deduced indirectly by considering the results achieved on specimens molded at low and high injection speeds (v_{inj} = 6 and 150 mm/s), respectively. It was found that the effect of the skin-core structure is markedly stronger under uniaxial in-plane (i.e., ITI) than in biaxial out-of-plane type loading (i.e., IFWI). © 1999 John Wiley & Sons, Inc. J Appl Polym Sci 73: 1205–1214, 1999

Key words: injection molding; instrumented falling weight impact; isotactic polypropylene; molecular weight; skin-core morphology; instrumented tensile impact; α-phase; β-phase; melt flow index

INTRODUCTION

Isotactic polypropylene (PP) homopolymers are widely used as raw materials for injection molding of various parts. In order to enhance the moderate toughness of PP below its glass transition temperature ($T_g \approx 0$°C), propylene is usually copolymerized with ethylene[1,2] or is blended with various rubbers.[3] Both of these techniques are associated, however, with a considerable loss in the stiffness and strength characteristics. It was early noticed that the β-phase PP (β-PP) outperforms the α-PP with respect to toughness.[4] Impetus to the development with β-PP was given only recently when highly selective β-nucleants became available.[5] Works have been devoted to the comparison of the fracture behavior of α- and β-PP produced by compression-,[6,7] injection-,[8–11] and extrusion-molding,[12] and other processing techniques.[13] Further, the effects of injection molding conditions on the morphology of α- (e.g., Refs. 14 and 15) and β-PP[10,14,16] were also the topic of numerous investigations. Interestingly, less information is available on how the in-plane[17–19] and out-of-plane[19] impact responses of α- and β-PP are affected by the skin-core mor-

Correspondence to: J. Karger-Kocsis (E-mail: karger@ivw.uni-kl.de).

Contract grant sponsor: German Science Foundation; contract grant number: DFG Ka 1202/4-1.

Contract grant sponsor: Volkswagen Foundation; contract grant number: I/7068.

Journal of Applied Polymer Science, Vol. 73, 1205–1214 (1999)

 CCC 0021-8995/99/071205-10

Table I MFI and Molecular Characteristics of the PP Homopolymers Studied

PP Grade	Code	MFI (dg/min)	M_w (kg/mol)	P (−)
Tipplen H384	α-H3	13.4	219	3.0
Tipplen H543	α-H5	5.5	268	4.1
Tipplen H781	α-H7	0.76	441	3.4

phology. A further open question is how the molecular weight (MW) of the β-nucleated PP resin affects the fracture performance. Fujiyama reported in his pioneering work[11] that the toughness of the β-PP increases with decreasing melt flow index (MFI) or increasing MW. Based on Izod test results, he has shown that the toughness improvement by β-nucleation diminishes with increasing MFI.[11] Our intention was to contribute to the still unsolved topics listed above. Therefore this paper was aimed at comparing the instrumented tensile (ITI, in-plane fracture) and falling weight impact (IFWI, out-of-plane fracture) response of α- and β-PPs that were injection molded of PP resins with various MFI. In order to study the effects of the molding-induced skin-core structure, specimens were molded by various injection speeds.

EXPERIMENTAL

Materials, Processing, and Characterization

Three commercial isotactic PP homopolymer grades (Tipplen PP types of Tisza Chemical Works Ltd., Tiszújváros, Hungary) with varying MFI (230°C/2.16 kg) and thus with different MW characteristics were involved in this study. When molded, all of them crystallize in the α-modification form. Data on the MFI, weight average MW (M_w) and polydispersity (P) of the PPs along with their designation used in the text are summarized in Table I.

The β-iPP was produced by adding the calcium salt of pimelic acid (according to the Hungarian patent 209 132) in 0.1 wt % to the related base PP–resin prior to the injection molding operation. The β-nucleant was dispersed in the PP melt by a Brabender Plasticorder twin-screw extruder at 200°C. Plaques with the dimension of 60 × 60 × 2 mm^3 were injection molded on an Engel ES 200/50 HL machine (screw diameter 30 mm) by setting melt and mold temperatures at 240 and 80°C, respectively. The high mold temperature was selected to favor the development of the β-PP.[16] In order to study the effect of the injection molding induced morphology, plaques were molded at two injection speeds, viz. v_{inj} = 6 and 150 mm/s. Note that v_{inj} strongly influences the thickness of the skin layer in the molded items.[14,16,19]

The molding-induced skin-core structure was studied by polarized light microscopy (PLM). Thin sections of ca. 10 μm were sliced across the plaque thickness by a Leitz microtome and viewed in PLM. The β-content of the plaques was determined by the method of Turner-Jones et al.[20] based on the related wide-angle X-ray spectra (WAXS). WAXS patterns were taken from the core after removing the molding-induced skin layers by polishing (300 μm from each side). WAXS was performed in a Phillips Micro Müller 111 device by using Ni-filtered CuK_a radiation.

Specimen Preparation, Testing, and Data Reduction

Two different testing procedures were adopted to investigate the effects of the α- and β-phase crystallinity and molding-induced microstructure: in-

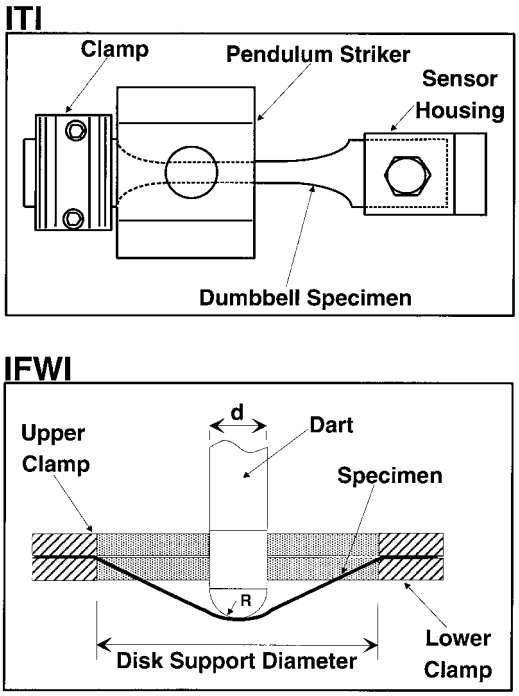

Figure 1 Schematics on the test setup of ITI and IFWI, respectively.

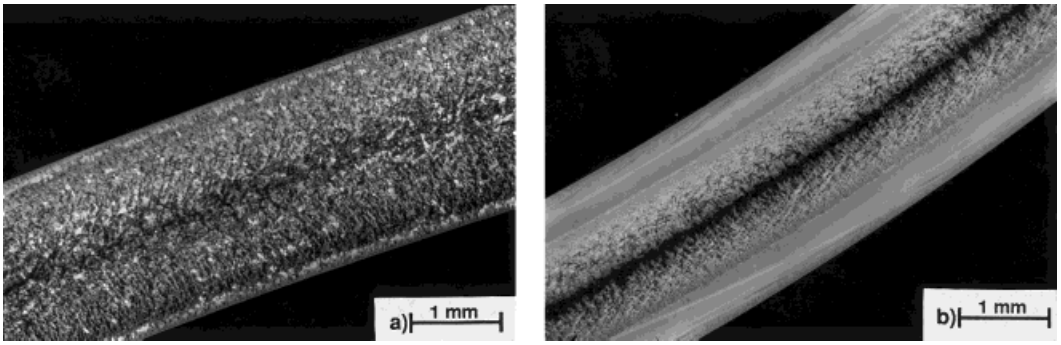

Figure 2 PLM pictures showing the injection molding-induced skin-core structure for α-PP as a function of MFI (v_{inj} = 6 mm/s). Designations: (a) α–H3 and (b) α–H7.

strumented tensile impact (ITI; according to DIN 53 448) and instrumented falling weight impact (IFWI). For ITI a pendulum (type 6545 of Ceast), whereas for IFWI a fall tower (Dartvis of Ceast) were used. Type A dumbbells, according to DIN 53 448 for ITI, were punched from the plaques using a pneumatic stamping device of Ceast. The length axes of all dumbbell specimens were aligned in the melt flow direction. ITI tests were performed at room temperature (RT) with a striker speed of v = 3.7 m/s and mass of m = 2.174 kg. Recording of the loading history occurred by the AFS-MK4 (Ceast) data acquisition system. From the ITI tests, performed on 5 parallel specimens, the following data were derived: E-modulus, elongation at break (ε_B) and tensile impact energy (W_f). The fracture surfaces of selected broken specimens were inspected in a scanning electron microscope (SEM, Jeol 5400) after sputtering with Pt/Pd alloy.

The IFWI tests were carried out at RT on the as-molded plaques (60 × 60 mm^2). The plaques, clamped on a supporting rig of 40 mm diameter were impacted with a hemispherically tipped dart of 20 mm diameter at an incident speed of v = 10 m/s. The incident energy of the dart was 150 J (at an impactor mass of 3.0 kg). Perforation impact tests were also performed on 5 samples. From the IFWI fractograms the disc modulus (E_d), the maximum strength (σ_d), the thickness-related perforation energy (E_{perf}/t) along with the deflections at the maximum load and perforation (x_{max} and x_{perf}, respectively) were read or computed by the related data reductions[21]:

$$E_d = 0.145(1 - \nu^2)\left(\frac{\Delta F}{\Delta x}\right)\frac{D^2}{t^3} \quad (1)$$

$$\sigma_d = \frac{2.5F_{max}}{t^2} \quad (2)$$

where ν was Poisson's ratio (ν = 0.3 was presumed), $\Delta F/\Delta x$ the slope of the F–x trace, D the diameter of the disc support (=40 mm), t the thickness of the sheet, and F_{max} the maximum

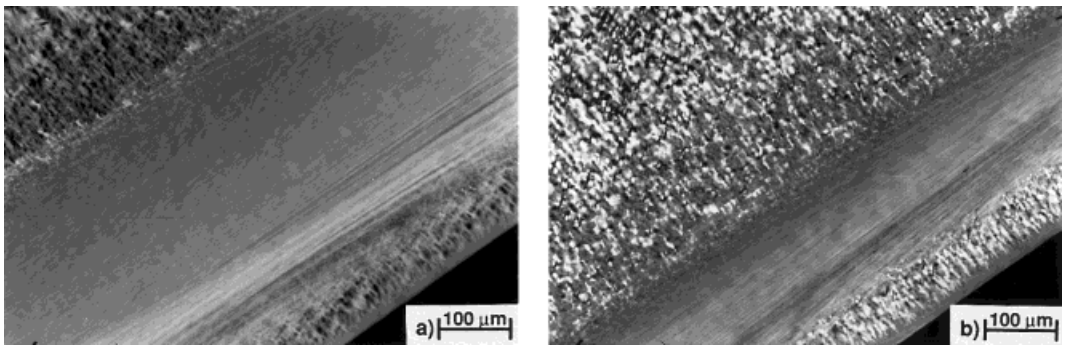

Figure 3 PLM pictures showing the injection molding-induced skin-core structure developed by v_{inj} = 150 mm/s for α- and β-PP, respectively (MFI ≈ 0.8 dg/min). Designations: (a) α–H7 and (b) β–H7.

Table II Change in the Core β-Content and Skin Thickness as a Function of MFI and Injection Speed (v_{inj})

	β-Content in Core, k (−) v_{inj} (mm/s)		Skin Thickness[a] (μm) v_{inj} (mm/s)	
PP	6	150	6	150
α-H3	—	—	60–70	60–70
β-H3	0.89	0.94	60	60
α-H5	—	—	130	110
β-H5	0.89	0.93	120	100
α-H7	—	—	350–400	250
β-H7	0.83	0.92	250–300	200

[a] Varies with the distance from the gate.

load registered. The setup of the ITI and IFWI is depicted schematically in Figure 1.

RESULTS AND DISCUSSION

Effects of MFI and Injection-Speed on the Skin-Core Structure

Figure 2 shows PLM pictures taken from the α-PP plaques molded from the resins of the highest and lowest MFI at v_{inj} = 6 mm/s. One can see that the skin thickness increases with increasing MW or decreasing MFI. Increasing v_{inj} resulted in a thinner overall skin. The skin thickness was also affected by the MFI of the PP: the skin layer enlarged by decreasing MFI. These findings are in concert with results of earlier studies.[14–16,19,22] The skin layer thickness of the β-nucleated samples was similar to the α-PP at high MFI, but became thinner with decreasing MFI when compared to the α-PP (see Figure 3). Figure 3 displays the complex structure of the skin layer. Varga et al.[23] recently distinguished three sublayers in the skin of these specimens (from the surface toward the core): a transcrystalline zone at the mold wall (due to nucleation by the cold wall), a spherulitic region (generated by plastic deformation of a stagnant melt layer), and a cylindritic layer (caused by severe melt shearing).

As the relative skin thickness is smaller in β-H3 than in β-H7 specimens, the overall β-crystallinity is higher for the PP version of high MFI. This is in harmony with the results of Fujiyama.[11] Data related to the skin-core morphology of the tested specimens are summarized in Table II.

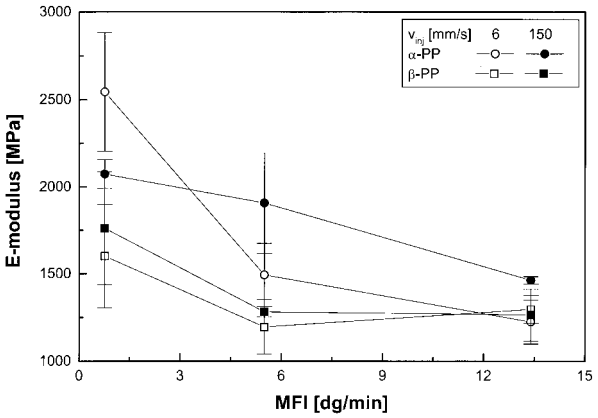

Figure 4 E vs. MFI functions as derived from the ITI tests for α- and β-PPs molded by various v_{inj}.

ITI Properties

Effects of Crystalline Phase

Figure 4 compares the E-modulus of the injection-molded α- and β-PPs as a function of MFI for samples produced with both v_{inj} = 6 and 150 mm/s, respectively. It can be observed that the stiffness of α-PP is superior to the β-PP, especially at low MFI. This finding correlates with results published for α- and β-PP in the literature.[7] In contrast, W_f of β-PP is markedly higher than α-PP (Figure 5). This is not surprising since increasing stiffness usually correlates with decreasing toughness and vice versa. The difference between β- and α-PP increases with decreasing

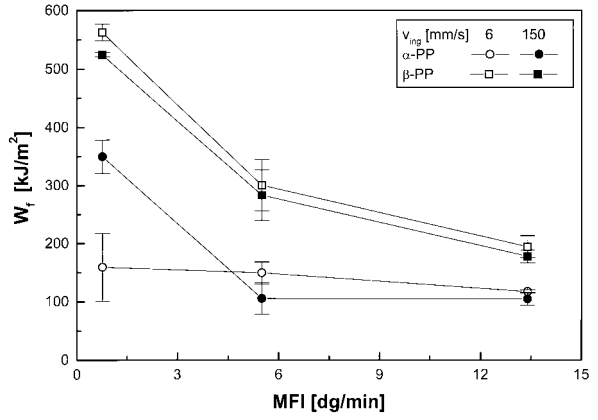

Figure 5 W_f vs. MFI functions as derived from the ITI tests for α- and β-PPs molded by various v_{inj}.

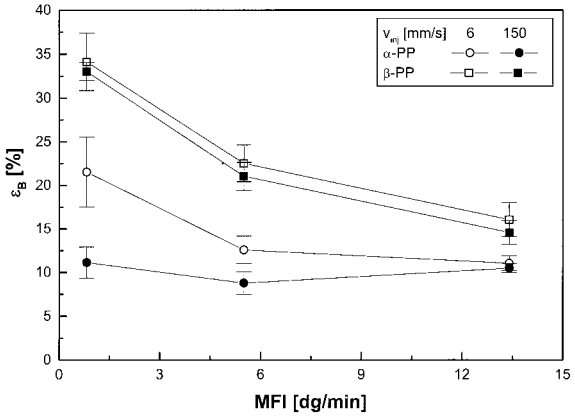

Figure 6 ε_B vs. MFI functions as derived from the ITI tests for α- and β-PPs molded by various v_{inj}.

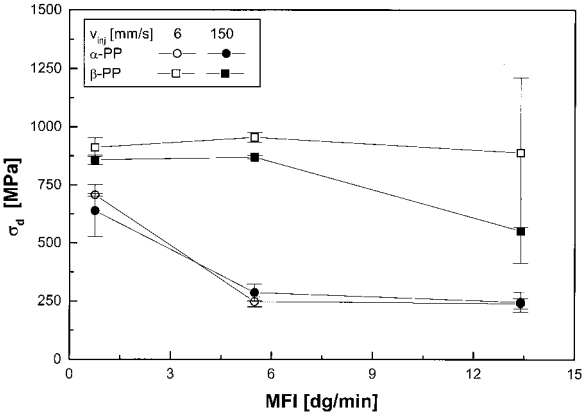

Figure 8 σ_d vs MFI functions as derived from the IFWI tests for α- and β-PPs molded by various v_{inj}.

MFI or increasing MW (see Figure 5). The ε_B vs. MFI data (cf. Figure 6) reflect the high ductility of β-PP compared to the α-version. The course of the W_f vs MFI (cf. Figure 5) follows a similar trend as that of ε_b vs MFI (cf. Figure 6). This was predictable since the total work of fracture usually changes parallel with the ultimate fracture strain.

The aforementioned results seem to support that the controlling parameter of toughness is not the β-phase crystallinity itself, but likely the MFI (or MW) of the β-nucleated PP. This finding corroborates the results of Fujiyama,[11] which were confirmed recently by Varga et al.[16] It should be kept in mind that the above results encounter also possible effects of the skin-core morphology. It is therefore of great importance to estimate the effects of the latter.

Effects of Skin-Core Structure

In order to elucidate the influence of the skin-core structure on the impact response it is straightforward to compare the results obtained on the α-H7 and β-H7 systems. The related data in Figure 4 show that the E-modulus of α-H7 decreases, whereas that of the β-H7 increases with increasing v_{inj}. This change is likely a complex effect of skin-shear-core morphology, skin thickness and orientation, and internal stress state.

The opposite tendency, as found for the E-modulus, can be predicted for the α- and β-H7 PP grades with respect to the W_f and ε_B data (cf. Figures 5 and 6). This was the trend, in fact, irrespective to some deviation related to α-H7. Interestingly the W_f and ε_B data were insensitive to the v_{inj} change for β-H7 PP samples (cf. Figures 5 and 6).

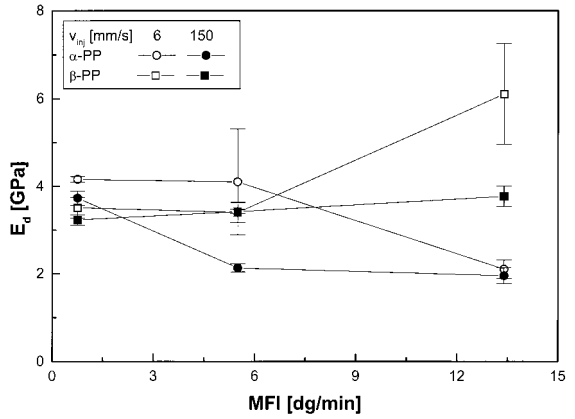

Figure 7 E_d vs. MFI functions as derived from the IFWI tests for α- and β-PPs molded by various v_{inj}.

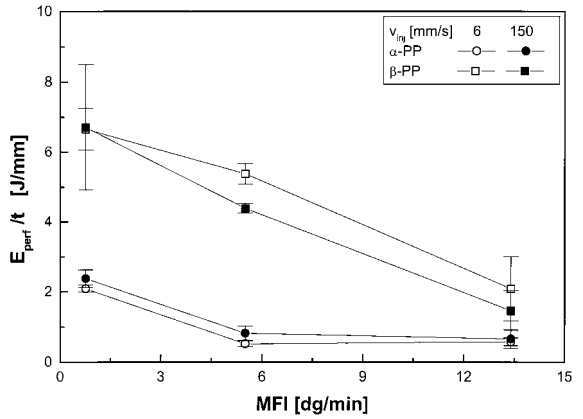

Figure 9 E_{perf}/t vs. MFI functions as derived from the IFWI tests for α- and β-PPs molded by various v_{inj}.

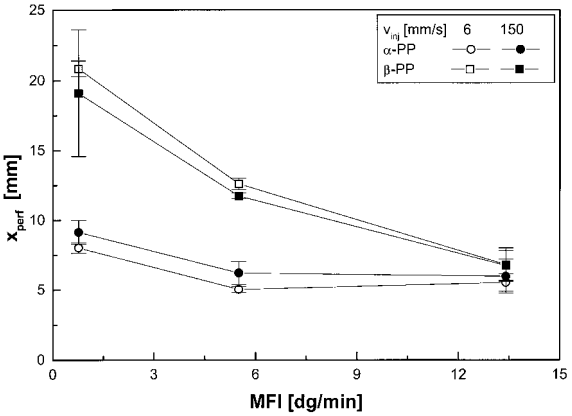

Figure 10 The x_{perf} vs. MFI functions as derived from the IFWI tests for α- and α-PPs molded by various v_{inj}.

It was reported for rubber-modified PP that the weak site of the skin-core structure is the intermediate layer between them, viz. the shear zone.[24] Obviously, the shear region becomes more pronounced with increasing v_{inj} and thus may result in a premature fracture. This scenario is likely reflected in the W_f and ε_B data of α-H7 when data at v_{inj} = 6 and 150 mm/s are compared (cf. Figures 5 and 6). β-PP, on the other hand, is less sensitive to changes in the skin-core structure.

IFWI Properties

Before discussing the experimental results attention should be drawn to the fact that ITI reflects the uniaxial in-plane fracture behavior while IFWI is a measure of the biaxial out-of-plane performance of the materials.

Effects of Crystalline Phase

E_d values calculated by eq. (1) decrease with increasing MFI for α-PP but remain practically constant for β-PP (Figure 7). The large scatter indicated for some samples seems to depend on the fracture mode (superposition of radial and circumferential cracking—see later). The apparent maximum strength σ_d [cf. Eq. (2)], is considerably higher for β-PP than for α-PP (Figure 8). This trend holds also for the deflection at maximum load (x_{max}). The thickness-related perforation impact energy (E_{perf}/t) vs MFI and x_{perf} vs MFI traces (Figures 9 and 10, respectively) demonstrate the steep increase of the impact resistance with decreasing MFI. Note that both perforation impact energy (Figure 9) and ductility of β-PP (Figure 10) are always superior to the α-PP.

The IFWI results correlate with those of the ITI. The only difference is that the outstanding impact performance of β-PP can also be observed in IFWI at higher MFI values. This suggests that β-PP is more resistant to fracture when biaxial loading conditions prevail. This finding is of great practical importance since biaxial loading of injection-molded parts is more frequent in the reality than the uniaxial one.

Effects of Skin-Core Structure

Collating the results inserted in Figures 7–10 for α-H7 and β-H7 one can conclude that the molding-induced skin-core structure affects the IFWI response only marginally. Recall that this finding was extracted from results achieved on samples molded by different v_{inj}. Note that various v_{inj} results in different skin-core morphology and thus internal stress state. Their effects, if any, seem to be overwritten by the experimental (material- and testing-related) scatter. The effects of morphology can perhaps be better studied on specimens with removed skin layers (now in

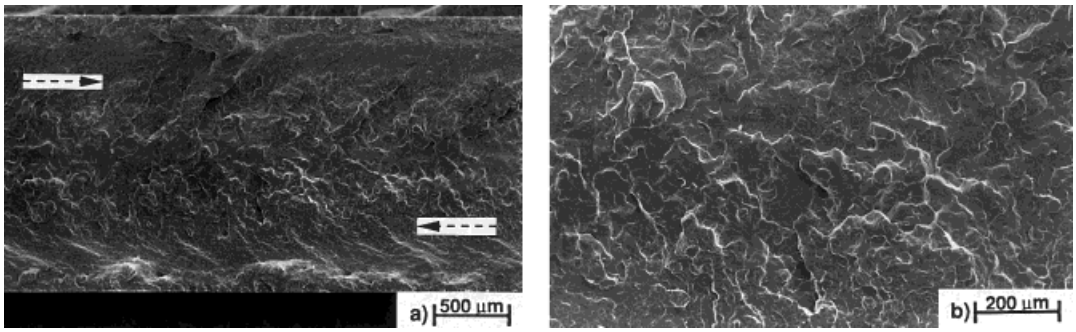

Figure 11 SEM photomicrographs taken on the ITI fracture surface of an α-H7 PP dumbbell molded by v_{inj} = 6 mm/s. Designations: (a) overview of the fracture surface and (b) core region.

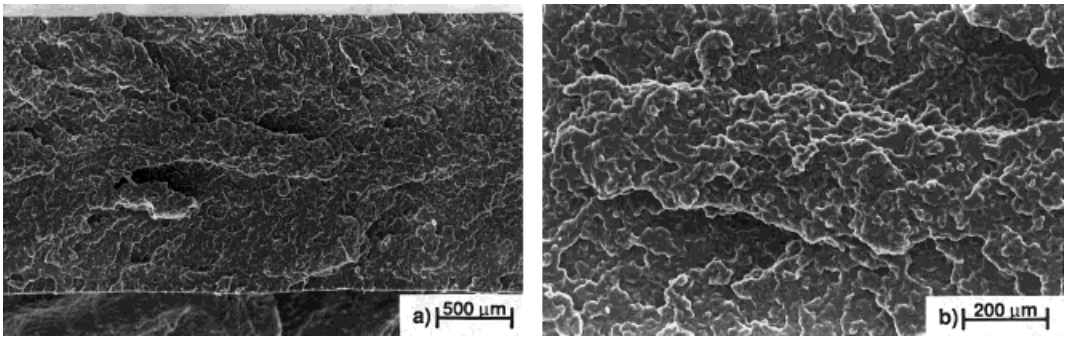

Figure 12 SEM photomicrographs taken on the ITI fracture surface of a β-H7 PP dumbbell molded by v_{inj} = 6 mm/s. Designations: (a) overview of the fracture surface and (b) core region.

progress) or on specimens produced by compression-molding.

Fractography

Selected scanning electron microscopy (SEM) pictures in Figures 11 and 12 show the fracture surfaces of ITI specimens α-H7 and β-H7 produced at the same v_{inj} (=6 mm/s). On the fracture surface of α-H7 the skin region can be well resolved (see Figure 11a). Further, based on the crack growth pattern one can even substantiate that cracking started in the subskin layer (i.e., shear zone—arrow indicates), as suggested in Ref. 24. The core layer is rather smooth with some patchy appearance (Figure 11b). By contrast, hardly any skin layer is apparent on the fracture surface of β-H7 (Figure 12a). This suggests that the failure modes in the skin and core layers are similar in β-PP. The core region of β-H7 shows a pronounced "patchwork-type" surface topography. The latter is a clear hint that some crazing preceded the final fast fracture.[25] If it is so, craze remnants should be found at high magnification. This is the case, in fact, as Figure 13 displays. The sponge-like and fibrillar structure observed for β-H7 is completely missing for the α-H7 PP. The spongy structure is a direct evidence for crazing in PP.[26,27] On the other hand, the appearance of fibrils (also observed by Tjong et al.[8]) may be attributed to the tie molecules within (intra) and between (inter) the β-spherulites. This assumption is based on the fact that the tie molecule density increases with increasing MW.[28] The spongy surface pattern may also be relied on the β-to-α transition demonstrated for β-phase PP both under static and dynamic loading conditions by using differential scanning calorimetry (DSC),[6,7,29] X-ray,[30] and microhardness[31] measurements. This transition is associated per se with voiding since it is accompanied by volume contraction. Recall that the crystalline density of

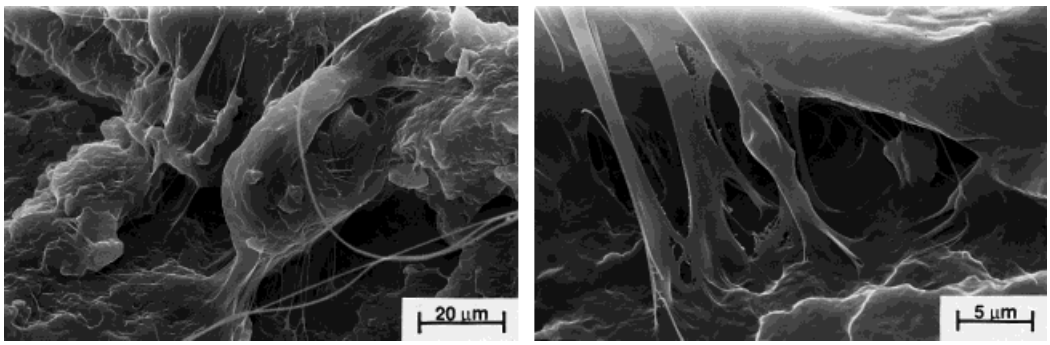

Figure 13 High magnification SEM pictures taken from the core region of an ITI β-H7 PP specimen.

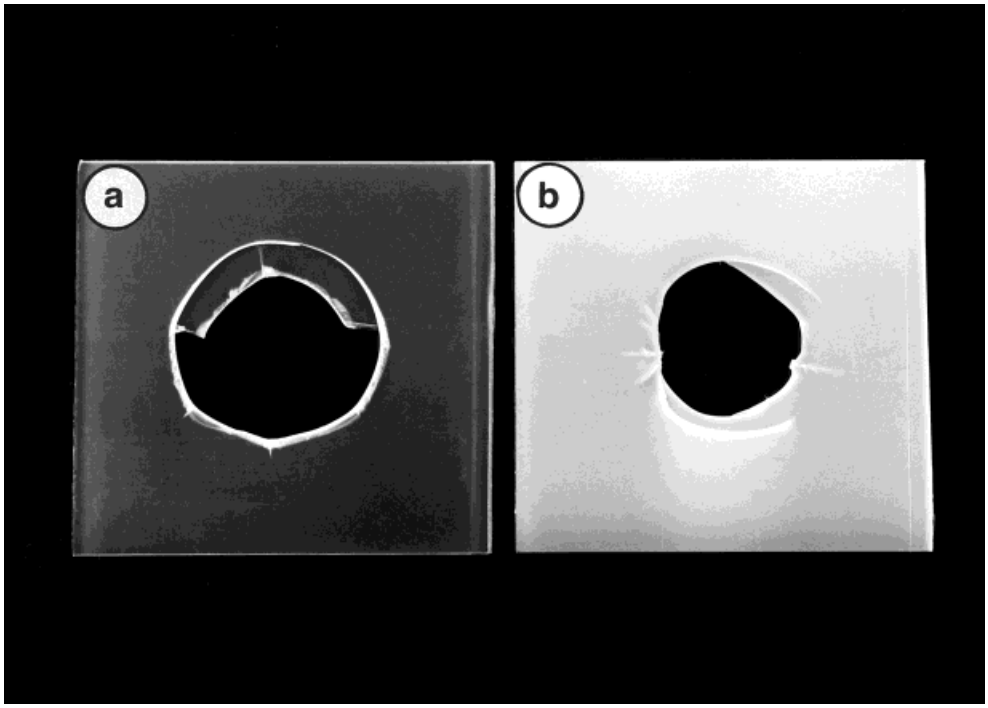

Figure 14 Comparison of the IFWI perforation behavior of (a) α-H3 and (b) β-H3 PP plates molded by v_{inj} = 6 mm/s.

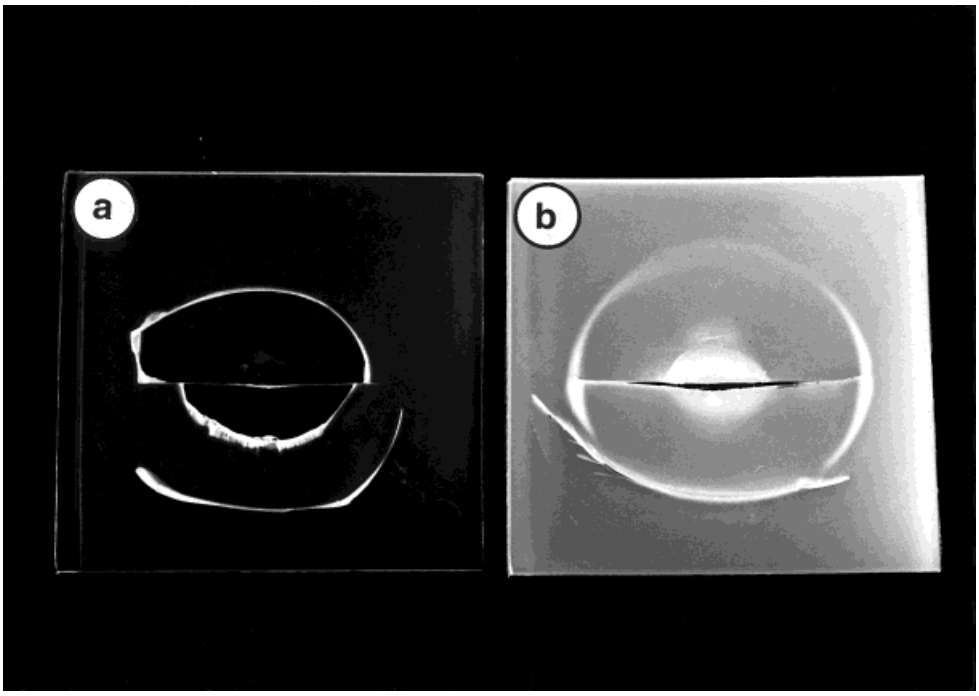

Figure 15 Comparison of the IFWI perforation behavior of (a) α-H7 and (b) β-H7 PP plates molded by v_{inj} = 150 mm/s.

the α-form is higher than that of the β-modification.[5,32]

As far as what the failure under perforation concerns: both the appearance and hole size of the samples in IFWI changed as a function of MFI. The fracture mode of the α- and β-PP plates is rather similar at high MFI (Figure 14). At lower MFI, on the other hand, the failure scenario changes substantially—viz., bending along the clamping ring becomes obvious (Figure 15). The β-H7 plate failed by single splitting (along the MFD as expected) at high bending, which caused some frictional deceleration of the impactor. This yielded a stress whitened area in which β-to-α phase transition could be revealed by DSC. For the α-H7 plate splitting accompanied with circumferential cracking were found to precede the penetration of the impactor.

CONCLUSIONS

This study was focused on ITI (uniaxial, in-plane loading) and IFWI (biaxial, out-of-plane loading) behavior of injection-molded α- and β-PP homopolymers having various MFI's and thus MW's. The following conclusions can be drawn from the test results:

1. The impact resistance of β-PP is superior to the α-version. The difference between α- and β-PP increased with decreasing MFI (or increasing MW). The β-content decreased with increasing MW due to the development of thicker skin layers composed of the α-modification. This finding suggests that the toughness of β-iPP is likely controlled by the MW characteristics of the PP rather than by the β-phase content of the nucleated PP itself.
2. The effect of the skin-core structure on the fracture response was deduced from results achieved on samples which were molded by various injection speeds (v_{inj}). In contrast to β-PP, the injection molding-induced skin-core structure strongly affected the ITI response of α-PP, especially at low MFI. On the other hand, the IFWI properties of both α- and β-PP were not significantly influenced by the skin-core morphology.
3. Fractographic inspection of the ITI specimens suggested that the outstanding fracture resistance of β-PP is related to a dense intra- and interspherulitic tie molecule density.

The authors gratefully acknowledge the support of the German Science (DFG Ka 1202/4-1) and Volkswagen Foundations (I/7068), respectively. Thanks are also to Prof. Bodor (TU Budapest) for the WAXS measurements.

REFERENCES

1. Galli, P.; Haylock, J. C.; Simonazzi, T. In Polypropylene: Structure, Blends and Composites; Karger-Kocsis, J., Ed.; Chapman and Hall: London, 1995; Vol 2, p. 1.
2. Suhm, J.; Schneider, M. J.; Mülhaupt, R. In Polypropylene: An A-Z Reference; Karger-Kocsis, J., Ed.; Kluwer Academic: Dordrecht, 1999; p. 104.
3. Martuscelli, E. In Polypropylene: Structure, Blends and Composites; Karger-Kocsis, J., Ed.; Chapman and Hall: London, 1995; Vol 2, p. 95.
4. Jacoby, P.; Bersted, B. H.; Kissel, W. J.; Smith, C. E. J Polym Sci B Phys 1986, 24, 461.
5. Varga, J.; Ehrenstein, G. W. In Polypropylene: An A-Z Reference; Karger-Kocsis, J.. Ed.; Kluwer Academic: Dordrecht, 1999, p. 51.
6. Karger-Kocsis, J. Polym Eng Sci 1996, 36, 203.
7. Karger-Kocsis, J.; Varga, J. J Appl Polym Sci 1996, 62, 291.
8. Tjong, S. C.; Shen, J. S.; Li, R. K. Y. Polymer 1996, 37, 2309.
9. Karger-Kocsis, J.; Varga, J.; Ehrenstein, G. W. J Appl Polym Sci 1997, 64, 2057.
10. Fujiyama, M. Intern Polym Process 1995, 10, 172.
11. Fujiyama, M. Intern Polym Process 1995, 10, 251.
12. Karger-Kocsis, J.; Putnoki, I.; Schöpf, A. Plast Rubb Compos Process Appl 1997, 26, 372.
13. Fujiyama, M. Intern Polym Process 1996, 11, 159.
14. Fujiyama, M. In Polypropylene: An A-Z Reference; Karger-Kocsis, J., Ed.; Kluwer Academic: Dordrecht, 1999, p. 668.
15. Mencik, Z.; Fitchmun, D. R. J Polym Sci Phys 1973, 11, 973.
16. Varga, J.; Mudra, I.; Ehrenstein, G. W. SPE ANTEC Tech Papers 1998, 44, 3492.
17. Fujiyama, M.; Azuma, K. J Appl Polym Sci 1979, 23, 2807.
18. Viana, J. C.; Cunha, A. M.; Billon, N. Polym Eng Sci, 1999, in press.
19. Cunha, A. M.; Pouzada, A. S.; Crawford, R. J. Plast Rubb Compos Process Appl 1992, 18, 79.
20. Turner Jones, A.; Aizlewood, J. M.; Beckett, D. R. Makromol Chem 1964, 75, 134.
21. Jones, D. P.; Leach, D. C.; Moore, D. R. Plast Rubb Process Appl 1986, 6, 67.

22. Tartari, D.; Bramuzzo, M. Kunststoffe, 1993, 83, 460.
23. Varga, J.; Breining, A.; Ehrenstein, G. W.; Bodor, G. Intern Polym Process, in press.
24. Karger-Kocsis, J.; Csikai, I. Polym Eng Sci 1987, 27, 241.
25. Michler, G. H. Kunststoff-Mikromechanik; Hanser: München, 1992.
26. Karger-Kocsis, J.; Friedrich, K. Intern J Fatigue 1989, 11, 161.
27. Narisawa, I.; Ishikawa, M. In Series Adv Polym Sci 91/92, Crazing in Polymers; H.-H. Kausch, Ed.; Springer: Berlin, 1990; p. 353.
28. Karger-Kocsis, J. Macromol Symp, 1999, in press.
29. Karger-Kocsis, J.; Shang, P. P.J Thermal Anal 1998, 51, 237.
30. Riekel, C.; Karger-Kocsis, J. Polymer, 1999, 40, 541.
31. Krumova, M.; Karger-Kocsis, J.; Baltá-Calleja, F. J.; Fakirov, S. J Mater Sci, 1999, in press.
32. Varga, J. In Polypropylene: Structure, Blends and Composites; Karger-Kocsis, J., Ed.; Chapman and Hall: London, 1995; Vol 1, p. 56.